Power System Technology
ISSN:1000-3673

Received: 16-01-2025 Revised: 05-02-2025 Accepted: 22-03-2025

# Advanced Design and Implementation of Modified SEPIC Converter Integrated with Grid Connected PV System: Performance Evaluation under Various Environmental Conditions

**Sanjay Nayak[1], Vivek Gupta[2], Maninder Kaur[2]**

*1University Institute of Engineering & Technology, Panjab University, Chandigarh*

*2 University School of Electrical & Electronics Communication Engineering Rayat Bahra University, Mohali, Punjab, India*

***Abstract:-*** The escalating popularity of solar energy, propelled by environmental consciousness, government initiatives, and its inherent accessibility underscores a pivotal shift towards sustainable power sources. However, the seamless integration of solar energy into the utility grid remains a formidable challenge for researchers. This complexity arises from multifaceted factors encompassing electrical apparatus, DC/AC conversions, diverse voltage levels, adherence to complex grid codes, and the imperative for precision in modeling techniques. In response to these challenges, this research paper propounds a dynamic model designed to mitigate the integration issues between photovoltaic (PV) systems and the grid. The model comprises of solar PV array, VSC (Voltage Source Inverter), DC-DC boost converter, transformer, LCL filter, and associated control circuitry. One of the significant contributions involves designing and implementing a modified SEPIC boost converter for the system. Through MATLAB simulations, the study showcases substantial enhancement in both efficiency and overall performance when compared to the conventional dc-dc boost converter.

***Keywords****: Modified SEPIC converter, dc-dc boost converter, Overall performance, and high efficiency, Photovoltaic (PV) system.*

## 1. Introduction

The continuous utilization of non-renewable energy resources like oil as well as coal contributes significantly to environmental issues like pollution and climate variation. In disparity, renewable energy sources which as solar & wind power offer promising solutions to mitigate these challenges and are also abundantly available in nature. In a country like India, solar energy derived from photovoltaic systems stands out as a viable future energy source, it not only addresses the challenges of increased energy demands but also contributes to mitigating global warming. The merits of PV energy include: it's free from reliance on fuel, pollution-free, noise-free, and abundantly available in nature with an extensive lifespan [1-10].

However, integrating solar energy into the electric grid is not that simple, requires specific steps to be carefully considered. Conventional DC-DC boost converters are employed with the system to elevate the voltage levels but encounter limitations such as low efficiency, large

Power System Technology
ISSN:1000-3673
Received: 16-01-2025 Revised: 05-02-2025 Accepted: 22-03-2025

conduction loss, and higher gain of voltage [11]. The design along with control of the dc-dc boost converter must account for changes in sun irradiance and temperature to ensure a constant voltage supply to the load. The SEPIC (Single Ended Primary Inductor Converter) is also used to amplify the voltage, the capability of handling non-inverting voltage conversions, ensuring consistent output voltage even during fluctuating input sets it apart from conventional DC-DC boost converters. The main PV array component is a solar cell, essentially a p-n junction semiconductor material. When the light from the sun hits this junction, it generates electricity. The generation of electricity directly depends on the rate of photo-current. However, there is some resistance in the electron's path as it flows through the PV array [12-13]. Hence the PV array output continuously varies with changes in sun irradiance and temperature. Therefore, it becomes essential to ensure a constant voltage supply to the load through careful design & control of the DC-DC boost converter. [14]. To achieve high efficiency, the DC-DC boost converter design is a major consideration in PV array grid-connected systems [15]. Advanced converters like modified SEPIC converters have demonstrated superior adaptability to reduce voltage oscillations and maintain low current ripple, resulting in high efficiency even when the PV array receives dynamic irradiance [16-19].

## 2. Objectives

The schematic diagram represented by Fig. 1 displays the essential components of grid grid-connected PV array system. These components comprise a DC-DC boost converter, a PV array, a filter, a transformer, and the grid itself. To ensure optimal efficiency and minimal distortion in DC voltage conversion, it is important to accurately model different components of the system and understand their characteristics and dynamic performance. Conventional DC-DC boost converters which are buck, boost & buck-boost typically require high duty cycle to generate higher output voltages leading to high switching voltage stress and increased ripple in the inductor currents, which adversely impact both conversion efficiency and voltage gain [20-21]. Hence, designing a suitable DC-DC boost converter is necessary that can effectively control output voltage, like a modified SEPIC converter that minimizes voltage stress during switching and provides higher conversion efficiency by employing advanced techniques for stable output under varying conditions.

Power System Technology
ISSN:1000-3673
Received: 16-01-2025 Revised: 05-02-2025 Accepted: 22-03-2025

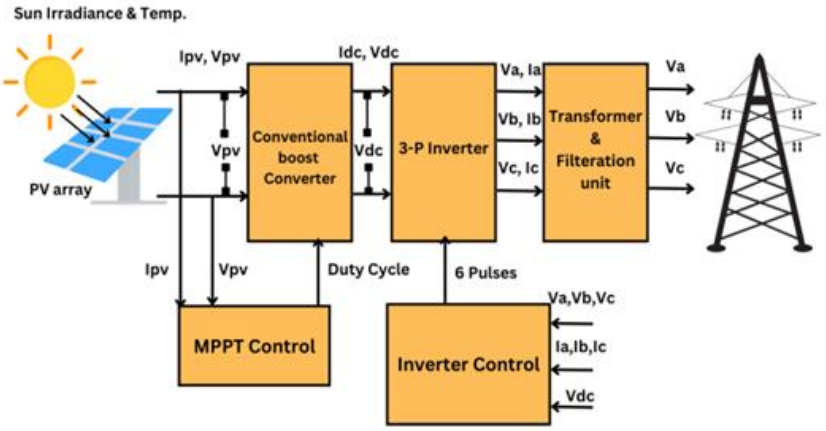


**Fig. 1 Schematic diagram of grid-connected array with a conventional boost converter**

### a. PV array

The PV array's mathematical model is constructed using a single diode equal circuit that represents the PV cell behavior as represented in the Fig. 2.

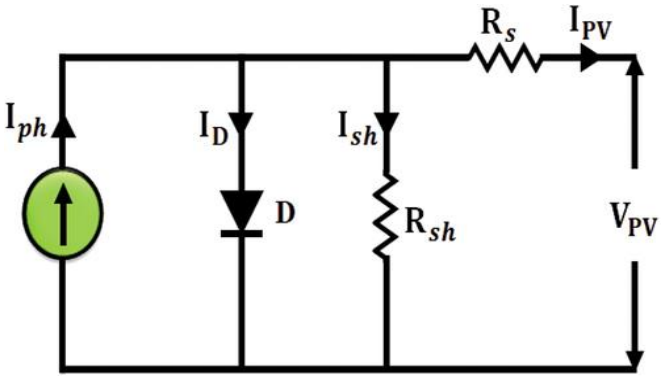


**Fig. 2 Equivalent circuit of a single PV cell.**

Eq (1) defines the output current of a PV cell as the difference between photon current and diode current. The practical cell also includes series and shunt resistance which can be seen in Fig. 2.

$$I_{PV} = I_{ph} - I_d - I_{sh} \qquad (1)$$

$$I_d = I_s \left(e^{\frac{q(V_{PV}+R_S I)}{mKT}} - 1\right) \qquad (2)$$

Power System Technology
ISSN:1000-3673
Received: 16-01-2025 Revised: 05-02-2025 Accepted: 22-03-2025

$$I_{sh} = \frac{V_{PV}+IR_s}{R_{sh}} \quad (3)$$

By putting (2) and (3) in (1), $I_{PV}$ can be given as:

$$I_{PV} = I_{ph} - I_s\left(e^{\frac{q(V_{PV}+R_sI)}{mKT}} - 1\right) - \frac{V_{PV}+IR_s}{R_{sh}} \quad (4)$$

The photovoltaic cell's output power $P_{PV}$ has been provided by:

$$P_{PV} = V_{PV}I_{PV} \quad (5)$$

- ***PV Cell Characteristics***

Integrating equations (1)-(5), a mathematical model for the PV array has been developed, considering the number of series & parallel cells along with their associated resistive losses.

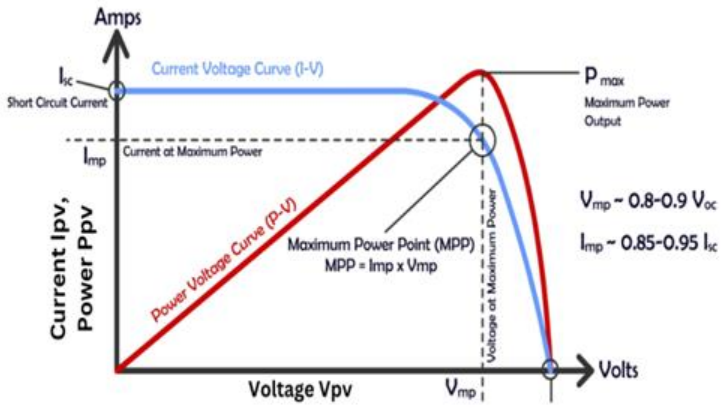


**Fig. 3 Current, Power, and Voltage characteristics of PV cell**

### b. DC-DC Boost Converter

The circuit depicted in Fig. 4 is specially designed for continuous conduction mode, operating in a cyclic manner between two separate loops. During the "ON" state of the switch, the inductor current increases, storing energy within it. Simultaneously, capacitor C discharges through the load resistor R, following a specific relationship:

$$L\frac{di_L}{dt} = V_{PV} \quad (6)$$

$$C\frac{dV_{dc}}{dt} = \frac{V_{dc}}{R} \quad (7)$$

Power System Technology
ISSN:1000-3673
Received: 16-01-2025 Revised: 05-02-2025 Accepted: 22-03-2025

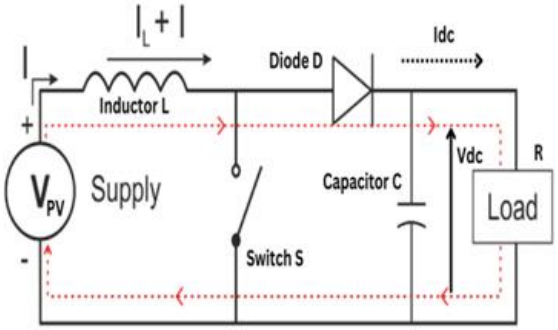


**Fig. 4 Conventional DC-DC boost converter**

On the other hand, when we turn "OFF" the switch, the inductor initiates the transferring of its energy to the load leading to discharge. Simultaneously, the voltage across the output capacitor rises. These changes could be mathematically described using the following equations:

$$L\frac{di_L}{dt} = V_{PV} - V_{dc} \qquad (8)$$

$$C\frac{dV_{dc}}{dt} = i_L - \frac{V_{dc}}{R} \qquad (9)$$

The duty cycle in a boost converter determines how long the switch remains ON relative to the overall period of switching. A longer "ON" time results in improved energy stored in the inductor, leading to a greater energy transfer to the capacitor during the "OFF" period. Consequently, a higher capacitor output voltage enhances the conversion efficiency. Therefore, adjusting the duty cycle enables control over the conversion effectiveness of the boost converter and could be derived from the ratio of "the output & input voltage.

$$\text{Duty cycle, } d = \frac{V_{PV} - V_{dc}}{V_{dc}} \qquad (10)$$

***c.*** *Modified SEPIC Converter*

The modified SEPIC converter is designed by integrating the components of a conventional SEPIC converter, a conventional DC-DC boost converter, and a" diode-capacitor circuit. The modified SEPIC converter provides high efficiency, minimal current oscillation, reduced voltage stress during switching, and significantly reduced conduction losses [19].

Power System Technology
ISSN:1000-3673
Received: 16-01-2025 Revised: 05-02-2025 Accepted: 22-03-2025

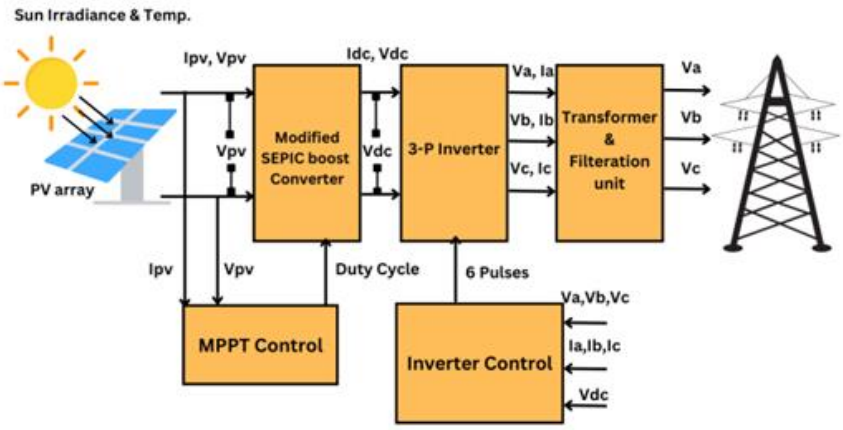


**Fig.5 Schematic diagram of grid-connected array Modified SEPIC boost converter**

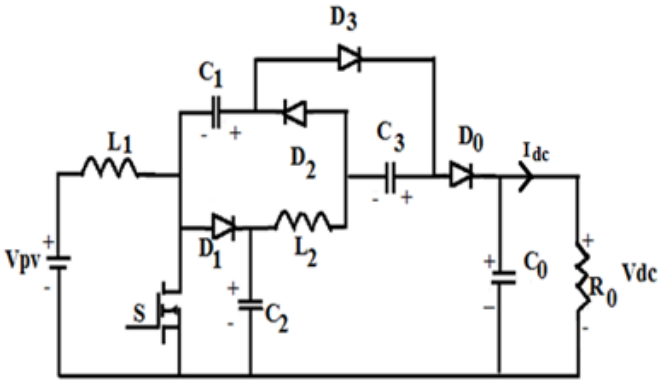


**Fig. 6 Circuit diagram of proposed modified SEPIC converter.**

- $V_{PV}$ denotes the input voltage that is 273V
- $V_{dc}$ denotes the output voltage that is 500V
- $f_s$ denotes the fundamental frequency that is $5 \times 10^3$Hz
- $D$ denotes the duty cycle for "the modified SEPIC converter
- $d$ denotes the duty cycle for a conventional DC-DC boost converter"
- $\Delta V_c$ denotes voltage ripple on the capacitor $C_1$, $C_2$, $C_3$
- $\Delta i_{L1,2}$ denotes the ripple current on the inductor $L_1$, $L_2$
- $L_1$, $L_2$ denotes the inductance of a modified SEPIC converter
- $C_1$, $C_2$, $C_3$ denotes the capacitance of a modified SEPIC converter

Power System Technology
ISSN:1000-3673

Received: 16-01-2025 Revised: 05-02-2025 Accepted: 22-03-2025

The addition of a diode-capacitor circuit, low-voltage MOSFETs, and low resistance helps to decrease the switching stress across MOSFETs and diodes. By reducing switching stress, the conversion effectiveness of the suggested model is increased. Therefore, the suggested model is suitable for renewable energy-based systems operating on lower input dc voltage. The circuit topology in Fig. 6 showcases the proposed converter design, which includes various components like a dc voltage source $V_{dc}$ , a primary switch S, 3 diodes ($D_1$, $D_2$, and $D_3$), 3 capacitors ($C_1$, $C_2$, and $C_3$), 2 inductors ($L_1$and $L_2$), output diode$D_0$, & output capacitor $C_0$. During the conduction phase, the voltage is transferred from the capacitor $C_2$to the inductor$L_2$, increases the gain of voltage of a suggested modified SEPIC converter model in comparison to the conventional dc-dc boost converter [22].

- ***Parameter Calculation for Proposed Model Table1.0***

| *Parameters to be calculated* | *Conventional Converter [22]* | *Modified Converter [21]* |
|---|---|---|
| *Duty cycle* | $d = 1 - \frac{V_{PV}}{V_{dc}}$ | $D = \frac{2V_{dc} - 3V_{PV}}{2V_{dc} + V_{PV}}$ |
| *Inductors* | $L_1 = \frac{V_{dc}d}{\Delta i_L f_s}$ | $L_2 = \frac{V_{PV}D}{\Delta i_{L1} f_s}$<br>$L_2 = \frac{V_{c2}(1-D)}{\Delta i_{L2} f_s}$ |
| *Capacitors* | $C = \frac{d}{R\frac{V_{dc}}{V_{PV}} f_s}$ | $C_1 = C_2 = C_3 = \frac{I_{dc}}{\Delta V_c f_s}$ |

- ***Calculated parameters value Table 2.0***

| *Calculated Parameters* | *Parameter's Value* |
|---|---|
| *Duty Cycle* | $D = 0.1$ |
| *Inductors* | $L_1 = 1.9 \times 10^{-3}\, H$<br>$L_2 = 25.4 \times 10^{-3} H$ |

Power System Technology
ISSN:1000-3673
Received: 16-01-2025 Revised: 05-02-2025 Accepted: 22-03-2025

| | |
|---|---|
| *Capacitors* | $C_1 = 3.3 \times 10^{-6} F$<br>$C_2 = 3.3 \times 10^{-6} F$<br>$C_3 = 3.3 \times 10^{-6} F$ |

### *d. Three Phase Inverter*

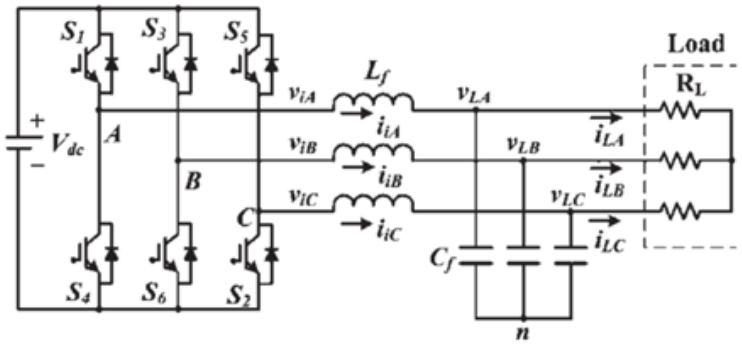


**Fig. 7 Three-phase inverter.**

3 single-phase inverter switches make up a 3-phase inverter, which is utilized for converting the converter's DC output voltage to an AC voltage. These switches are controlled in such a coordinated manner that every switch operates at every 60-degree point of the fundamental output waveform. As a result, forms a six-step line-to-line output waveform. In order to remove harmonics with multiples of three, the output waveform has a 0-step voltage among the square waveform positive along negative sections. Furthermore, by applying the SPWM technique to six-step waveform the waveform's overall shape is preserved

## 1. Control Mechanism of Proposed System

- ***MPPT Control Mechanism***

From the power-voltage curve of the PV cell, it can be concluded that there exists an optimal operating point at which max power could be delivered to the load. This point needs to be regulated at regular intervals as the operating point varies with the difference in solar irradiation along with cell temp [23]. The control mechanism of the operating point has been depicted in the Fig. 8.

Power System Technology
ISSN:1000-3673
Received: 16-01-2025 Revised: 05-02-2025 Accepted: 22-03-2025

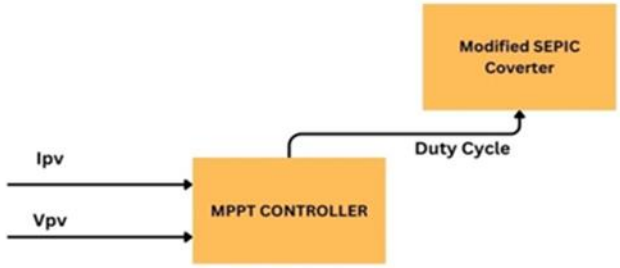


**Fig. 8 MPPT control mechanism for Modified SEPIC converter.**

- ***Incremental Conductance Method***

DC-DC boost converter & MPPT algorithm both play a crucial part in enhancing the overall PV array performance. The IC method involves two sensors, one for measuring the voltage and the other for measuring the PV array current output [24], which are used to enhance the efficiency of the PV array. Differentiating Equation (5) w.r.t voltage yields the following equation:

$$\frac{dP_{PV}}{dV_{PV}} = V_{PV} \times \left(\frac{dI_{PV}}{dV_{PV}}\right) \quad (11)$$

$$\frac{dP_{PV}}{dV_{PV}} = I + V_{PV} \times \left(\frac{dI_{PV}}{dV_{PV}}\right) \quad (12)$$

The above equation satisfies the condition of max power point tracking, substituting the condition in Eq. 11, the equation becomes:

$$\frac{dI_{PV}}{dV_{PV}} = -\left(\frac{I_{PV}}{V_{PV}}\right) \quad (13)$$

Fig. 9 can be better understood by the following equations

At "MPP:

$$\frac{dI_{PV}}{dV_{PV}} = -\frac{I_{PV}}{V_{PV}} \quad (14)$$

Left of MPP:

$$\frac{dI_{PV}}{dV_{PV}} > -\frac{I_{PV}}{V_{PV}} \quad (15)$$

Right of MPP

$$\frac{dI_{PV}}{dV_{PV}} < -\frac{I_{PV}}{V_{PV}} \quad (16)$$

Power System Technology
ISSN:1000-3673
Received: 16-01-2025 Revised: 05-02-2025 Accepted: 22-03-2025

The equation $\frac{dI_{PV}}{dV_{PV}} > -\frac{I_{PV}}{V_{PV}}$ signifies the PV module incremental conductance on the left side, while the right side $\frac{dI_{PV}}{dV_{PV}} < -\frac{I_{PV}}{V_{PV}}$ represents the instantaneous conductance". Furthermore, at $\frac{dI_{PV}}{dV_{PV}} = -(\frac{I_{PV}}{V_{PV}})$ the PV array will operate at the maximum power.

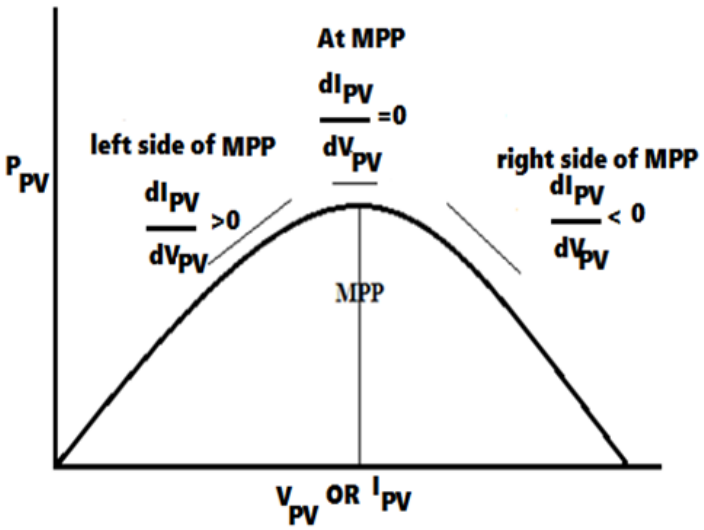


**Fig. 9 Incremental conduction realization**

$$\frac{dP_{PV}}{dV_{PV}} = 0$$

- ***Inverter Control Mechanism***

A 3-phase, 3-level inverter is designed using IGBT switches. The advantage of using IGBT semiconductor switches lies in their compact size and reduced switching losses when compared to other power electronic devices. The Voltage source converter (VSC) not only governs the DC bus voltage but also ensures a unity power factor. The control mechanism for the three-phase inverter is described in Figure 10 [26].

- ***DC Voltage Control***

The DC link capacitor plays an essential part in mitigating power losses at inverter IGBT switches, thereby providing real power. Therefore, the voltage at the DC link capacitor reduces gradually. To maintain stable voltage at the capacitor, the inverter absorbs a slight amount of the active power. This principle has been explored in various research studies [27-28].

Power System Technology
ISSN:1000-3673
Received: 16-01-2025 Revised: 05-02-2025 Accepted: 22-03-2025

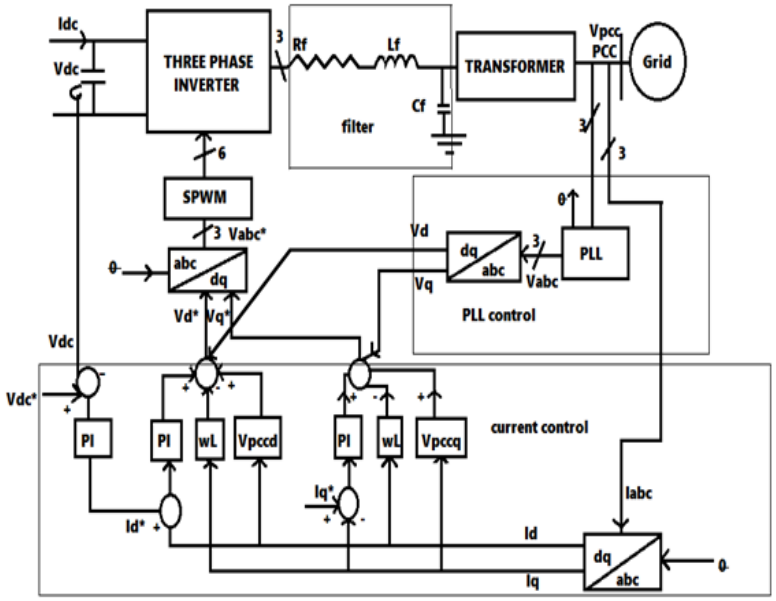


**Fig. 10 Three-phase inverter control mechanism.**

- ***Phase-locked loop technique***

To regulate the output voltage in power electronics systems, "the phase-locked loop (PLL) technique is generally utilized to synthesize the system's phase and frequency. The pulse width modulation (PWM) approach is used in conjunction with PLL. The q component of the PCC (Point of Common Coupling) voltage in the" dq-frame could be stated by the following equations:

$$V_{pcc-q} = \hat{V} \sin(\omega t + \theta_0 - \theta) \qquad (17)$$

To decouple the control of active along with reactive power, the regulation of $V_{pcc-q}$ is set to zero. The choice is rooted in the fact that active power control correlates with the real part of the output voltage, aligning with the voltage of a grid. While reactive power control corresponds to the imaginary part of the output voltage, which is 90 degrees out of phase with grid voltage. By regulating $V_{pcc-q}$ to zero, the output voltage retains only the in-phase component having a grid voltage, crucial for active power control, while eliminating the out-of-phase component. This enables precise control over reactive power alone. In the provided equation $\hat{V}$ signifies the amplitude of the PCC phase voltage, $\omega$ represents the frequency of system, and $\theta_0$ denotes the AC system's initial phase angle.

- ***Current control***

Dq frame's inverter currents are given by the equations provided below [28] [31]:

Power System Technology
ISSN:1000-3673
Received: 16-01-2025 Revised: 05-02-2025 Accepted: 22-03-2025

$$L_f \frac{di_d}{dt} = L_f \omega(t) i_q - R_f i_d + V_d - V_{pcc-d} \quad (18)$$

$$L_f \frac{di_q}{dt} = -L_f \omega(t) i_d - R_f i_q + V_q - V_{pcc-q} \quad (19)$$

Where $V_{pcc-dq}$ represents "point of common coupling voltages (PCC), $i_{dq}$ signifies the inverter current, $V_{dq}$ denotes the voltage at inverter's AC side in the dq-frame. In this context, a proportional-integral (PI) controller is implemented for each and every current component. The equations for active along with reactive power outputs of inverter in the dq-frame" have been provided by the following eq:

$$P(t) = \frac{3}{2}( V_q(t) i_d(t) + V_d(t) i_q(t) \quad (20)$$

$$Q(t) = \frac{3}{2} (-V_d(t) i_q(t) + V_q(t) i_d(t) ) \quad (21)$$

Because of the PLL operation $V_d = \hat{V}$ & $V_q = 0$.
The current controllers of the inverter receive reference values from the outer loops, which are determined by the operation mode and control objectives. The regulation of $i_d$ is responsible for controlling the inverter's active power output, whereas the regulation of $i_q$ governs the control of reactive power output.

## 1. RESULTS AND DISCUSSIONS

The present study conducts a comparative examination of the conventional and modified SEPIC boost converters, through the adept application of the Tustin/Backward Euler method within the MATLAB/SIMULINK environment. The simulations were executed, focusing on a PV array operating under standard test conditions, specifically at 25°C with an intended radiation of 1000 W/m$^2$ for a duration of 0.4 seconds. The scope of work extended to the Modified Single-Ended Primary Inductor Converter design based on the parameters outlined in theTable 1 and then the calculated values provided in Table 2. This design facilitated a comparative analysis, under identical standard test conditions.
The results encapsulated in Fig. 11-21, unveil the comparative dynamics of PV output voltage $V_{PV}$, PV output power $P_{PV}$, converter voltage $V_{dc}$, grid voltage $V_a$, grid current $I_a$ , total harmonic distortion (THD) analysis & the grid power (P) with respect to time. This research affords a detailed understanding of the distinctive performance characteristics exhibited by the two converter configurations.

Power System Technology
ISSN:1000-3673

Received: 16-01-2025 Revised: 05-02-2025 Accepted: 22-03-2025

## 1. COMPARATIVE ANALYSIS OF CONVENTIONAL AND PROPOSED SYSTEM

Fig. 11 illustrates that from 0 to 0.1 seconds, the PV power output $P_{PV}$ of the conventional converter exhibits ripples, while the modified SEPIC converter produces a smoother output. Furthermore, between 0.1 and 0.4 seconds, the modified SEPIC converter consistently outperforms the conventional boost converter in the terms of output power, highlighting the effectiveness of the modification in enhancing performance and stability. These observations provide valuable insights into optimizing photovoltaic energy conversion systems

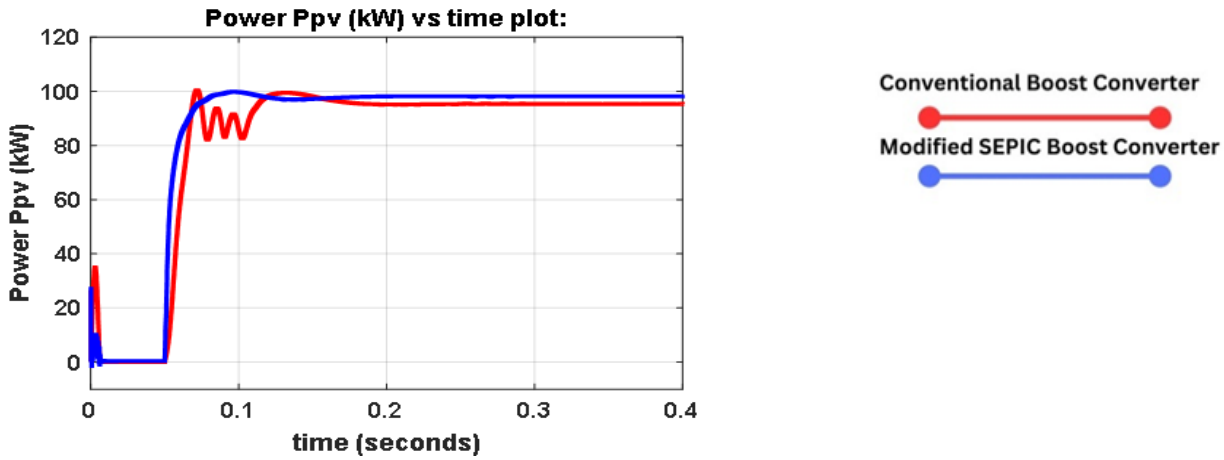


**Fig. 11 Comparative analysis of PV Power.**

In Fig. 12, the time period of 0-0.1seconds unveils that the "PV output voltage has ripples and transient voltage fluctuations in the case of a conventional DC-DC boost converter, conversely, the PV output" voltage from a modified SEPIC converter maintains a smooth profile and shows improved voltage regulation. Moreover, during the subsequent period from 0.1 to 0.4 seconds, the modified SEPIC converter PV output voltage is greater in comparison to that of traditional boost converter.

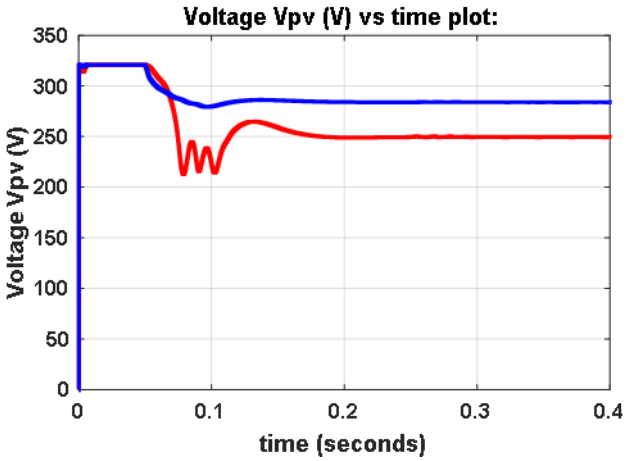


**Fig. 12 Comparative analysis of PV output voltage.**

Power System Technology
ISSN:1000-3673
Received: 16-01-2025 Revised: 05-02-2025 Accepted: 22-03-2025

In the “Fig. 13, it could be found that the designed converter exhibits achievement of voltage boosting to the desired level compared to the convention boost converter. Furthermore, the modified SEPIC” converter DC output voltage attains stability at an earlier instance as compared to the conventional converter, thereby contributing significantly to the effectiveness &stability of the total photovoltaic energy conversion system.

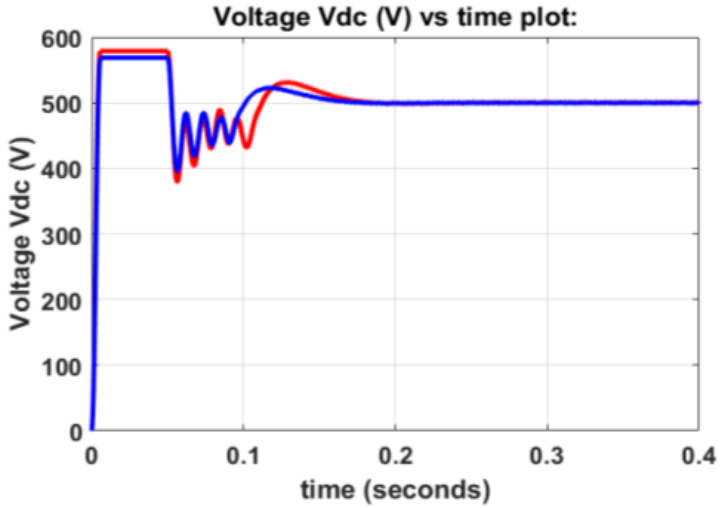


**Fig. 13 Comparative analysis of converter’s output voltage.**

Analysis of Fig.s 14 and 15 reveals a notable consistency in grid voltage $V_a$ between the conventional and modified SEPIC boost converters. The uniformity arises from the constant output voltage maintained by a three-phase inverter when supplied with DC voltage.

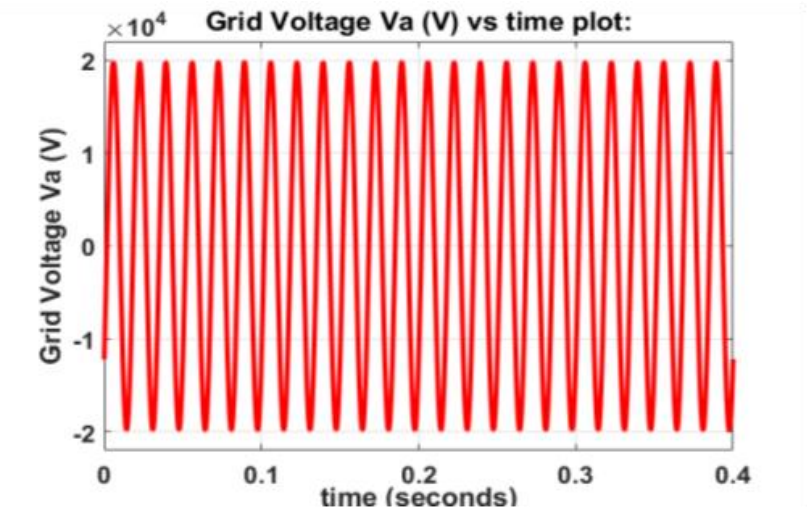


**Fig. 14 Grid voltage output in case of conventional boost converter.**

Power System Technology
ISSN:1000-3673
Received: 16-01-2025 Revised: 05-02-2025 Accepted: 22-03-2025

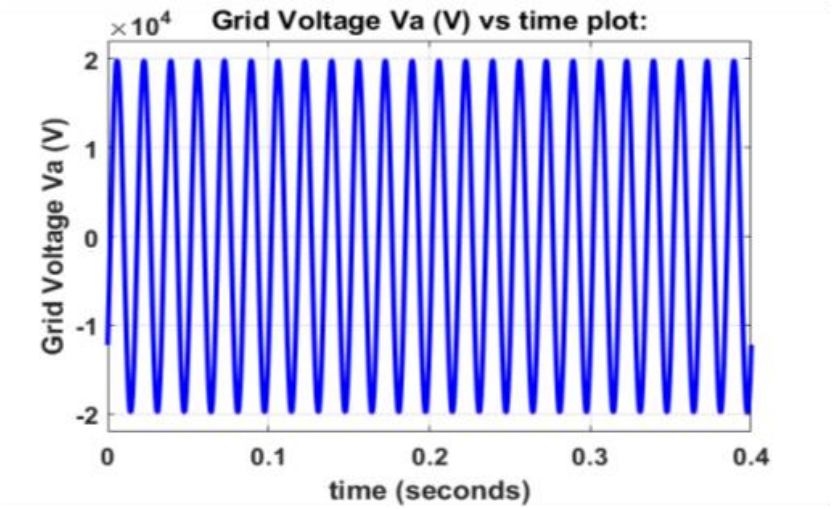


**Fig. 15 Grid voltage output in case of modified SEPIC boost converter**

Fig. 16 represents a comparison of the grid current $I_a$ , it can be observed that a higher current is fed into the grid in the case of a modified SEPIC boost converter.

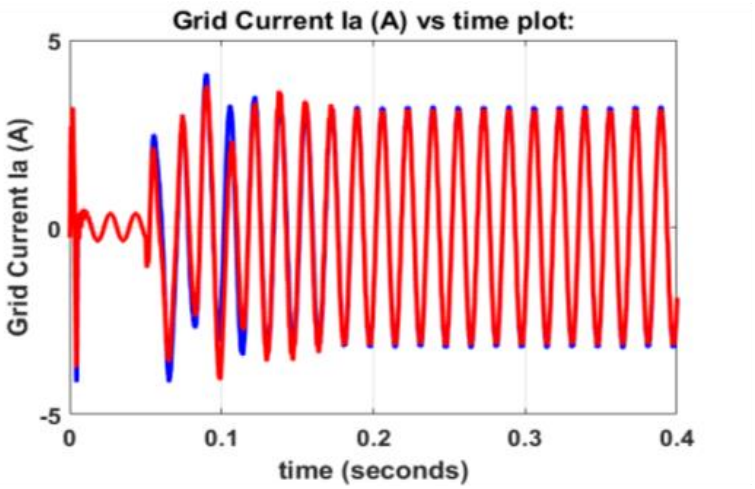


**Fig. 16 Comparative analysis of grid current.**

Figures 17 and 18 disclose a divergence in voltage characteristics at the interface between the converter and inverter, especially focusing on voltage distortion. The proposed converter exhibits a substantially lower distortion level $\Delta V_{dc} = 2.5\,V$ in difference to the conventional boost converter, where the distortion level is $\Delta V_{dc} = 5.1\,V$. In the case of a modified SEPIC converter, the reduced distortion contributes to an augmented performance of a 3-phase inverter. The mitigated distortion not only signifies improved signal but also the impact of

Power System Technology
ISSN:1000-3673
Received: 16-01-2025 Revised: 05-02-2025 Accepted: 22-03-2025

SEPIC converter design on inverter performance resulting in a smoother and more efficient power conversion process.

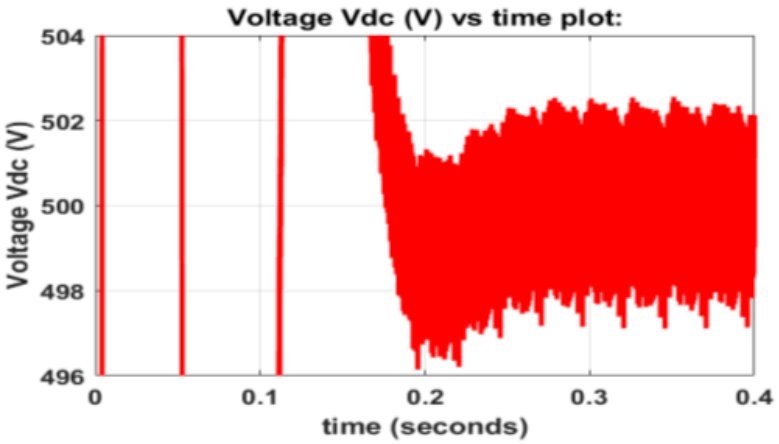


**Fig. 17 Voltage distortion in case of conventional boost converter.**

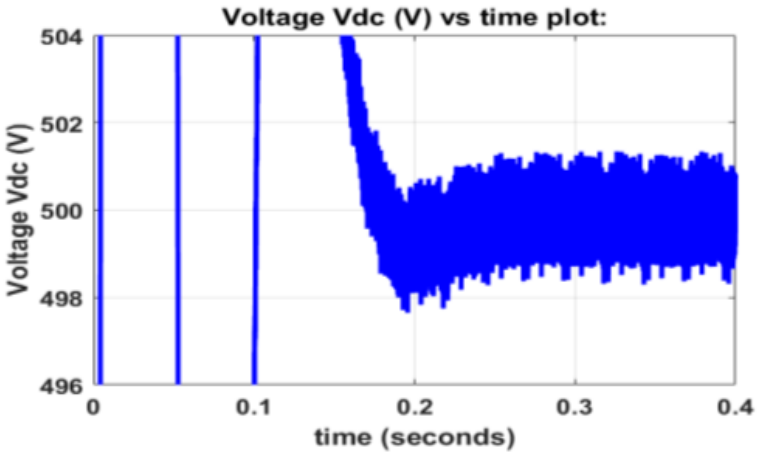


**Fig. 18 Voltage distortion in case of modified SEPIC boost converter.**

In Fig. 19, grid power (P) and efficiency comparison show that the power in the case of the modified SEPIC converter becomes stable prior and provides higher efficiency in contrast to the conventional boost converter. In time period 0.1-0.4, it could be found that the effectiveness of the conventional boost converter is 93.5% whereas, the effectiveness of the system with the suggested converter is 96.2%. In essence, the finding underscores the efficacy of the modified SEPIC converter in mitigating operational challenges and enhancing efficiency, thereby positioning it as a better option for grid-connected PV array systems, particularly during transient operation conditions

Power System Technology
ISSN:1000-3673
Received: 16-01-2025 Revised: 05-02-2025 Accepted: 22-03-2025

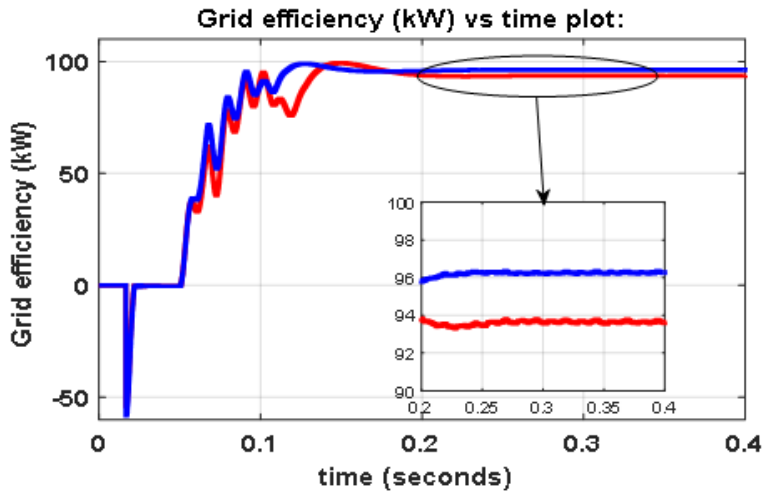


**Fig. 19 Comparative analysis of converter's efficiency.**

Figs. 20 and 21 present a comparative evaluation of the THD calculated on the grid side, providing critical insights into the harmonic content of both the conventional and modified converters. The analysis reveals an identical THD value of 0.33% for both converters. This consistent THD outcome suggests uniformity in the harmonic distortion characteristics on the grid side, irrespective of the converter configuration. The uniformity in THD values contributes valuable insights into the harmonic mitigation potential of modified SEPIC converters, offering a promising outlook for their application in grid-connected photovoltaic systems with a focus on harmonic reduction and grid code compliance.

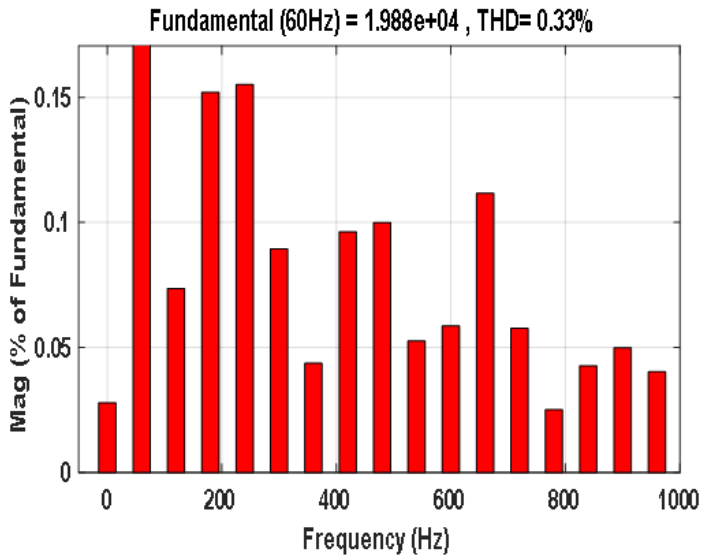


**Fig 20. THD in the case of the conventional boost converter.**

Power System Technology
ISSN:1000-3673
Received: 16-01-2025 Revised: 05-02-2025 Accepted: 22-03-2025

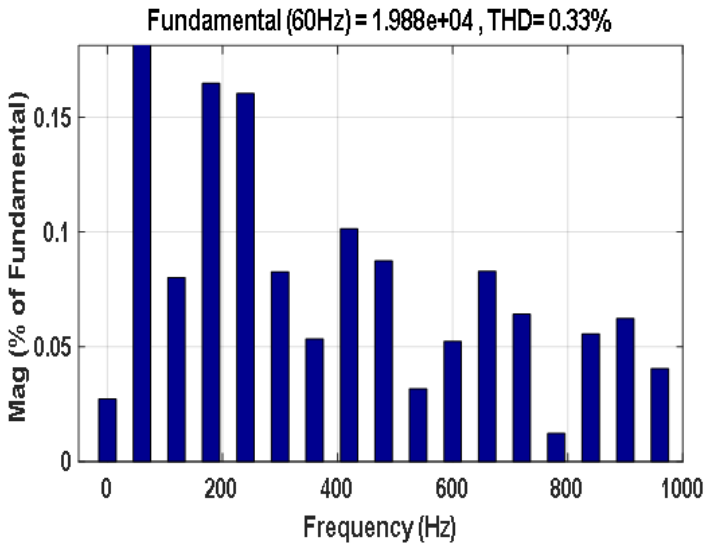


**Fig. 21 Total harmonic distortion in case of modified SEPIC boost converter.**

Furthermore, the performance of both converters can be analyzed on the basis of the calculated parameters provided in the given table

***Table 3.0***

| ***Serial No.*** | ***Parameters*** | ***Conventional converter*** | ***SEPIC converter*** |
|---|---|---|---|
| ***1.*** | *Variation in PV output voltage* $P_{PV}$ | *110 volts* | *40 volts* |
| ***2.*** | *Variation in the converter's output voltage distortion* $V_{dc}$ | *5.1 volts* | *2.5 volts* |
| ***3.*** | *Variation in efficiency* | *93.5%* | *96.2%* |
| ***4.*** | *Harmonic distortion (THD)* | *0.33%* | *0.33%* |

## 2. CONCLUSIONS

Moreover, with comprehensive modeling of the power circuit and its associated control circuitry within the grid-connected PV systems, this study draws several key conclusions:

Power System Technology
ISSN:1000-3673
Received: 16-01-2025 Revised: 05-02-2025 Accepted: 22-03-2025

1. Designed parameters for the modified SEPIC converter are specified as follows:
   Duty cycle (D): 0.1
   Inductor $L_1$ : $1.9 \times 10^{-3} H$
   Inductor $L_2$ : $25.4 \times 10^{-3} H$
   Capacitors $C_1, C_2, and\ C_3$: $3.3 \times 10^{-6} H$
2. The efficiency of the grid connected to the system of PV employing the conventional boost converter is measured at 93.5%, conversely, the same system when equipped with the designed boost converter, demonstrates an efficiency of 96.2%.
3. The system's voltage profile during the transient period with the proposed "modified SEPIC converter is improved compared to the system's voltage profile with the conventional DC-DC boost converter".

The THD of the voltage being fed to the utility grid is 0.33%, which is the same in the case of both converters.

**Refrences**

[1] Nehrir MH, Wang C, Strunz K, Aki H, Ramakumar R, Bing J, Miao Z, Salameh Z, "A review of hybrid renewable/alternative energy systems for electric power generation: Configurations, control and applications," *IEEE Trans. Sustain. Energy*, vol. 2, no. 4, pp. 392–403, Oct. 2011.

[2] Benjamin Kroposki, Robert Lasseter, Toshifumi Ise, S. Morozumi, S. Papathanassiou, and N. Hatziargyriou, "Making Microgrids Work", *IEEE Power and Energy Magazine*, vol.6, no.3, pp. 41-53, May-June 2008.

[3] Chi Kong Tse and Kevin M. Adams, "Qualitative analysis and control of a DC-to-DC Boost Converter Operating in Discontinuous Mode", *IEEE Transactions on Power Electronics*, Vol. 5, No. 3, pp 323-330, July 1999.

[4] Dieter K. Schroder, "Carrier Lifetimes in Silicon" *IEEE Transactions on electron devices*, 44 (1), pp 160- 170, Apr. 1997.

[5] Peyman Mazidi and G. N. Srinivas; "Reliability assessment of a distributed generation connected distribution system". International Journal of Power System Operation and Energy Management, 2011.

[6] Ministry of New and Renewable Energy, Government of India, "Annual Reports 2016-2017" , 2016, [Online], Available: http://mnre.gov.in/filemanager/annual-report/2016-2017/EN/pdf/1.pdf, [Accessed: July 6, 2017].

[7] "Ministry of New and Renewable Energy, Annual Report 2015-2016."

[8] Clemente Rodriguez, Gehan Amaratunga, "Dynamic stability of grid-connected photovoltaic systems," *IEEE Power Engineering Society General Meeting*, pp. 2193-2199, June 2004.

Power System Technology
ISSN:1000-3673

Received: 16-01-2025 Revised: 05-02-2025 Accepted: 22-03-2025

[9] Mohamad Reza Banaei and Hossein Ajdar Faeghi Bonab, ‘‘A novel structure for single-switch nonisolated transformerless buck–boost DC–DC converter,’’ IEEE Trans. Ind. Electron., vol. 64, no. 1, pp. 198–205, Jan. 2017.

[10] Coelho, Roberto F., Filipe Concer, and Denizar C. Martins. "A study of the basic DC-DC converters applied in maximum power point tracking." In Power Electronics Conference, 2009. COBEP'09. Brazilian, pp. 673- 678. IEEE, 2009.

[11] W. Li and X. He, “Review of non isolated high-step-up dc/dc converters in photovoltaic grid-connected applications”, IEEE Trans. Ind. Electron., vol. 58, no. 4, pp. 1239–1250, Apr-2011.

[12] Y.Tan, et al., “A model of PV generation suitable for stability analysis,” Energy conversion, IEEE Transactions on, vol.19, pp. 748-755,2004

[13] Marcelo Gradella Villalva and Jonas Rafael Gazoli, "Comprehensive approach to modeling and simulation of photovoltaic arrays," Power Electronics, IEEE Transactions on, vol. 24, pp. 1198- 1208,2009.

[14] Jong. Pil Lee, Byung-Duk Min, Tae-Jin Kim, Dong-Wookyoo and Ji-Yoon Yoo, “Input Series-output parallel connected DC/DC converter for a photovoltaic PCS with high efficiency under a wide load range”, Journal of Power Electronics, vol. 10, No.1, pp.9-13, January 2010.

[15] A.W.N. Husna, S.F. Siraj, M.Z. Ab Muin, “Modeling of DC-DC converter for solar energy system applications”, IEEE Symposium on Computers & Informatics, pp. 125-129, Mar. 2012.

[16] Daniel WH. Power Electronics. Indiana: McGraw-Hil. 2011: 144-150.

[17] Falin J. Designing DC / DC Converters Based on SEPIC Topology. Analog Appl J. 2008; 18–23.

[18] Kircioğlu O, Ünlü M, Çamur S. Modeling and Analysis of DC-DC SEPIC Converter with Coupled Inductors. 2016 International Symposium on Industrial Electronics, INDEL 2016 Proceedings. Bosnia Herzegovina. 2016: 1-5.

[19] Saravanan S, Babu NR. Design and Development of Single Switch High Step-up DC-DC Converter. IEEE J Emerg Sel Top Power Electron. 2017; 6(2): 855-863.

[20] Lung-Sheng Yang, Tsorng-Juu Liang, and J. F. Chen, “Transformer-less DC-DC converter with high voltage gain”, IEEE Trans. Ind. Electron., vol. 56, no. 8, pp. 3144–3152, Aug. 2009.

[21] R. Gules, W. M. Santos, F. A. Reis, E. F. R. Romaneli, and A. A Badin, “A modified SEPIC converter with high static gain for renewable applications,” IEEE Trans. Power Electron., vol. 29, no. 11, pp. 5860-5871, Nov. 2014.

[22] Daniel WH. Power Electronics. Indiana: McGraw-Hil. 2011: 144-150.

[23] Carl Ngai-Man Ho, Hannes Breuninger, SamiPettersson, Gerardo Escobar, Leonardo Augusto Serpa, and Antonio Coccia, “Practical design and implementation procedure

Power System Technology
ISSN:1000-3673

Received: 16-01-2025 Revised: 05-02-2025 Accepted: 22-03-2025

of an interleaved boost converter using SiC diodes for PV applications," IEEE Trans. on power electronics, vol.27, no. 6, June 2012.

[24] Azadeh Safari and Saad Mekhilef, "Simulation and Hardware implementation of incremental conductance MPPT with direct control method using Cuk converter", IEEE Trans.Ind. Electron., Vol. 58, no. 4, Apr. 2011, pp. 1154-1161.

[25] M. Veerachary, T. Senjyu, K. Uezato, (2002), "Voltage-based maximum power point tracking control of PV system", Aerospace and Electronic Systems, IEEE Transactions on ower electronics, vol. 38, no. 1, 2002, 262- 270.

[26] Linbin Huang, "A Virtual Synchronous Control for Voltage-Source Converters Utilizing Dynamics of DC-Link Capacitor to Realize Self Synchronization", IEEE J. Emerg. Sel. Top. Power Electron, vol. 5, no. 4, pp. 1565–1577, 2017.

[27] A. Yazdani and R. Iravani, Voltage-Sourced Converters in Power Systems: Modeling, Control, and Applications. New York, NY, USA: Wiley, 2010.

[28] A. Yazdani et al., "Modeling guidelines and a benchmark for power system simulation studies of three-phase single-stage photovoltaic systems," IEEE Trans. power delivery, vol. 26, no. 2, pp. 1247–1264, Apr. 2011.

[29] Best, Roland E. Phase-Locked Loops: Design, Simulation, and Application. McGraw-Hill, (Fifth Edition) 2003.